ISSN 2004-2965 Energy Proceedings, Vol. 23, 2021

International Conference on Applied Energy 2021
Nov. 29 - Dec. 5, 2021, Thailand/Virtual
Paper ID: 468

Least-cost hydrogen supply chain for off-site hydrogen production from large scale renewable power in China—A case study of China's Western Inner Mongolia

Luping HUO[1], Haiyang LIN [1,2], Qie SUN [1*]

1 Institute of Thermal Science and Technology, Shandong University, Jingshi Road No.17923, Jinan and 250061, China

2 John A. Paulson School of Engineering and Applied Sciences, Harvard University, Cambridge, MA 02138, USA

ABSTRACT

Concerting renewable energy into hydrogen and transporting it to the end of consumption is the promising choice to achieve large-scale deep decarbonization in transportation sector. Based on this, this paper constructs a large-scale centralized renewable energy hydrogen supply chain (HSC) network model to investigate the lowest cost of three different green hydrogen supply pathways, including production, compression, storage, transportation, and utilization. The fluctuation of wind power, solar power, and hydrogen fuel demand are integrated in the model, which is optimized by dynamic programming. Different production and delivery pathways are evaluated to find the least-cost way for transport hydrogen utilization. Applying the model to China's Western Inner Mongolia (WIM) region, the HSC network plan in 2030 was established. The results show that the least-cost hydrogen supply is to produce hydrogen by wind power and to transport it in liquid hydrogen by truck. This study provides guidance and reference for the future planning and design of green HSC network in other countries or regions.

Keywords: hydrogen supply chain, wind and solar power, delivery pathways, Western Inner Mongolia (WIM)

1. INTRODUCTION

The long-term dependence on and reckless use of fossil fuels has led to huge energy crisis and environmental problems. The transport sector is one of the major contributors of energy consumption (21%,2018) and greenhouse gas emissions (27%,2018) [1]. Hydrogen is considered as the most promising alternative energy for traditional fossil fuels, which can be used as a zero-emission power fuel for the transport sector to drive fuel cell electric vehicles. Nevertheless, one of the main obstacles to green hydrogen deployment is the lack of a large-scale, comprehensive and cost-effective HSC network.

To this end, many researchers have done a lot of research on the whole or part of renewable energy-based HSC and its related infrastructure, mainly focusing on the technical and economic analysis, scenario analysis, model optimization or evaluation. However, most HSC networks are evaluated based on multiple hydrogen production energy sources and a single supply route or a single hydrogen production energy source and multiple supply routes [2-4]. Generally, the assessment of hydrogen demand in the transport sector only considers light passenger vehicles, and does not take into account other types of vehicles (buses, trucks, etc.) [5, 6]. In addition, researches about technologies for large-scale H2 transport and storage have been done [7, 8]. However, none of the studies can fully consider the optimization design and operation of HSC with large-scale different renewable energy hydrogen production and supply pathways.

Accordingly, this paper proposes a large-scale renewable energy HSC network model considering different production and delivery pathways by dynamic planning of wind or solar power and hydrogen fuel demand to investigate the least-cost green hydrogen supply pathway for off-site hydrogen. Finally, the effectiveness of the model is verified by applying it to a case study based on China's WIM region in 2030.

2. METHODOLOGY

2.1 Hydrogen supply chain

The structure of the HSC is shown in Fig.1. HSC includes energy source, hydrogen production, storage, conversion, delivery, and dispensing. Two types of power resources are considered: wind and solar power on a utility scale. Hydrogen production technology is large-scale centralized water electrolysis. Considering the fluctuation and intermittence of wind and solar power, large-scale seasonal storage is needed near the production plant. The produced hydrogen is delivery or stored in the form of gas or liquid after conversion. The compressed gaseous hydrogen is delivery by tube trailer truck (GH2-Truck) or pipeline (GH2-Pipeline). Liquid hydrogen can be stored in super insulated spherical tank for a short time after liquefaction and transported by liquid hydrogen tank truck (LH2-Truck). Hydrogen is transported to the hydrogen refueling station for utilization. It's noted that the HSC is connected to the grid for necessary power supply, but the renewable power cannot be sold to the grid.

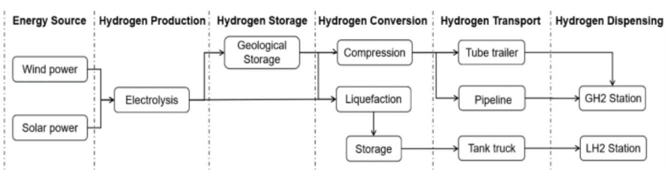

Fig. 1. Hydrogen supply chains. (GH2: Gaseous Hydrogen, LH2: liquid hydrogen)

2.2 Hydrogen demand estimation

The average daily hydrogen demand by region can be calculated with Formula (1).

$$HD_g = \sum_v p_{HFCV,v} N_v (\frac{D_v}{365}) FE_v , \quad \forall g \qquad (1)$$

where HD_g is the average daily hydrogen demand in the region g, kg / day; $p_{HFCV,v}$ represents the market penetration rate of hydrogen fuel cell vehicles (HFCV) in type v vehicles; N_v represents the number of vehicles in type v, D_v is the average annual driving distance km of v-type vehicle, and FE_v is the fuel economy kg/100km of v-type vehicle.

2.3 Technology description for HSC components

The following will briefly describe the technologies related to the components of HSC.

Production: In this study, the abundant wind and solar sources in WIM are used to hydrogen production by electrolysis. The alkaline electrolyzer (AEC) with mature technology, low cost and wide application was selected [9]. Two energy scenarios are considered: (I) utility scale wind power, (II) utility scale solar power.

Conversion: Considering the existing forms of GH2 and LH2, three conversion technologies, compression, liquefaction and pumps, are needed.

Delivery: Three ways of hydrogen transport were considered: GH2-Truck, LH2-Truck and GH2-Pipeline. Significantly, the key to evaluate the investment cost of truck transportation is to determine the number of trucks needed. The investment cost of pipeline transportation mainly depends on the diameter and length of pipeline.

Storage: In this study, salt cavern is used for large-scale hydrogen storage after production. Cryogenic liquid hydrogen storage tanks are used as buffer storage prior to truck transport.

Refueling: This paper estimates the cost of hydrogen refueling station based on HDSAM model and its own actual situation. It is assumed that the capacity of all hydrogen refueling stations are 1000kg/day and the supply pressure to the fuel cell tank is 70bar.

2.4 Hydrogen supply chain model

2.4.1 Objective function

Considering the fluctuation of wind or solar power and hydrogen demand, based on the least-cost of HSC network model, the HSC network costs of different hydrogen production and delivery pathways are optimized on the basis of hourly operation throughout a year.

The optimization model aims to minimize the total cost of the whole HSC network, which is calculated by dividing the total cost (C_{tot}), which includes annualized capital cost (C_{cap}), fixed operation cost (i.e. fixed operation and maintenance cost, C_{om}) and variable operation cost (C_{op}). C_{op} include the costs for freshwater (C_{wt}), truck fuel (C_{tf}), and grid electricity (C_{gd}), and offsetting revenue from selling by-product oxygen (C_{o2}). The objective equation and its expansion are as follows:

$$Min\ C_{tot} = C_{cap} + C_{om} + \left(C_{gd} + C_{wt} + C_{o2} + C_{tf}\right) \qquad (2)$$

$$\begin{cases} C_{cap} = \sum_{X=e}^{tr} \left(\alpha_X I_X \frac{i(1+i)^{T_X}}{(1+i)^{T_X}-1}\right) \\ C_{cap} = \sum_{X=e}^{tr} (\alpha_X \beta_X I_X) \\ X = [e; ec; cop; gs; lq; ls; lpu; tr] \end{cases} \qquad (3)$$

$$\begin{cases} C_{gd} = \gamma_{gd} \cdot \sum_{t=1}^{8760} P^t \\ C_{wt} = \gamma_{wt} \cdot r_{wt} \sum_{t=1}^{8760} H_{ec}^t \\ C_{o2} = \gamma_{o2} \cdot r_{o2} \sum_{t=1}^{8760} H_{ec}^t \\ C_{tf} = \gamma_{tf} \cdot r_{tf} \cdot n_{trip} \end{cases} \qquad (4)$$

Where α_X, β_X, I_X, and T_X denote the capital costs, O&M fractions, installed capacities, and lifetimes for wind or solar power (e), electrolyzers (ec), compressors (cop), geological storage (gs), liquefier (lq), LH2 storage (ls), LH2 pump (lpu), and trucks (tr), respectively. i is the interest rate. γ and r denotes the unit price and the demands for grid electricity(gd), freshwater(wat), oxygen(o2) and truck transport fuel(tf), respectively. P^t represents the amount of integrated grid power required at time t. The hydrogen output from the electrolysis system at time t are denoted by H_{ec}^t, n_{trip} represents the annual number of round trips.

2.4.2 Constraints

2.4.2.1 Power and hydrogen flow balances

For each time interval, electrolysis, conversion (compression, liquefaction, LH2 pump), hydrogen refueling station are balanced with wind or solar power generation and integrated grid power, shown as:

$$P_{ec}^t + (P_{cop}^t + P_{lq}^t + P_{lpu}^t) + P_{hs}^t = P_e^t + P_{grid}^t \quad (5)$$

The hydrogen flow constraints (Formual 6-16) take into account the hydrogen loss rate of each component of the HSC, shown as:

$$H_{ec}^t + H_{gs,dis}^t = H_{gs,cha}^t + H_{cov}^t \quad (6)$$

$$H_{p,cop}^t = H_{gs,cha}^t \quad (7)$$

$$H_{gs,cha}^t = H_{cov,gt}^t \quad (8)$$

$$H_{cov,gt}^t = \frac{H_{tr} \cdot n_{trip}}{8760 \cdot (1 - e_{l,cop})} \quad (9)$$

$$H_{cov,gp}^t = \frac{H_{pl}^t}{8760 \cdot (1 - e_{l,cop})} \quad (10)$$

$$H_{cov,lt}^t = \frac{H_{tr} \cdot n_{trip}}{8760 \cdot (1 - e_{ls}) \cdot (1 - e_{lpu})} \quad (11)$$

$$H_{lpu}^t = H_{ls,dis}^t + H_{ls,cha}^t \quad (12)$$

$$I_{ls} = t_{ls} \cdot \frac{H_{tr} \cdot n_{trip}}{8760 \cdot (1 - e_{ls}) \cdot (1 - e_{lpu})} \quad (13)$$

$$H_{tr} \cdot n_{trip} = \frac{\sum_{t=1}^{8760} H_{rf}^t}{(1 - e_{tr}) \cdot (1 - e_{rf})} \quad (14)$$

$$H_{pl}^t = \frac{\sum_{t=1}^{8760} H_{rf}^t}{(1 - e_{pl}) \cdot (1 - e_{rf})} \quad (15)$$

$$\sum_{t=1}^{8760} H_{rf}^t = AHD_{actual} \quad (16)$$

where $e_{l,cop}$, e_{ls}, e_{lpu}, e_{tr}, e_{pl} and e_{rf} indicate the loss rates for hydrogen during different conditioning processes. H^t indicate the hydrogen flowrate during different conditioning processes. H_{tr} is the payload of each truck. t_{ls} represents the time for LH2 storage. AHD_{actual} represents actual annual hydrogen demand of hydrogen refueling station, which depends on the hydrogen demand by region and the quality efficiency of each component.

2.4.2.2 Hydrogen demand constraints

Hydrogen demand during time t under hydrogen scenario e must be satisfied by local production and/or import from other regions as expressed in Eq. (17).

$$HD_{e,g}^t \le HP_{e,g}^t + \sum_{f,d} HQ_{e,f,d,g',g}^t, \ \forall g, e, t \quad (17)$$

where $HP_{e,g}^t$ is the hydrogen production rate by electrolyzers during time t in region g' under hydrogen scenario e; $HQ_{e,f,d,g',g}^t$ is the flowrate of hydrogen in form f via transport mode d from g' to g during time t in region g' under hydrogen scenario e.

2.4.2.3 Production constraints

- Power production

The wind or solar power P_e^t at time t is constrained by the installed capacity IC_e and the capacity factor CF^t at time t as follows:

$$0 \le P_e^t \le IC_e CF^t \quad (18)$$

- Hydrogen production

The hydrogen production rate of the electrolyzers is constrained by the minimum and maximum capacity and its number as follows:

$$HPCap^{min} N_g \le HP_{e,g}^t \le HPCap^{max} N_g, \quad \forall g, e, t \quad (19)$$

2.4.2.4 Storage constraints

The hydrogen charging and hydrogen discharging of geological storage are limited by the installed capacity of matching compressors. Liquid hydrogen charging and discharging is limited by the pump. The storage capacity of hydrogen is limited by the capacity of the applicable storage facilities. These constraints are as follows:

$$\begin{cases} 0 \le H_{s_f,cha}^t \le I_{dev} \\ 0 \le H_{s_f,dis}^t \le I_{dev} \\ 0 \le S_{s_f}^t \le I_{s_f} \\ S_{s_f}^{t+1} = S_{s_f}^t + e_{s_f,cha} \cdot H_{s_f,cha}^t - \dfrac{H_{s_f,dis}^t}{e_{s_f,dis}} - e_{s_f,self} \cdot S_{s_f}^t \\ S_{s_f}^1 = S_{s_f}^{8760} \end{cases} \quad (20)$$

where s_f represent geological storage or liquid hydrogen storage in form f. dev represent corresponding compressors or pumps. $e_{s_f,cha}$, $e_{s_f,dis}$ and $e_{s_f,self}$ represent the charging efficiency, discharging efficiency and self-discharge rate for gaseous hydrogen storage or liquid hydrogen storage, respectively.

2.4.2.5 Hydrogen transportation constraints

A minimum and maximum hydrogen flowrate is required in the transportation process to ensure that hydrogen flows from region g' to different regions g as follows:

$$\begin{cases} HQ_{f,d}^{min} X_{e,f,d,g',g}^t \le HQ_{e,f,d,g',g}^t \le HQ_{f,d}^{max} X_{e,f,d,g',g}^t \\ \forall t, e, f, d, g, g \ne g' \end{cases} \quad (21)$$

where $HQ_{f,d}^{min} X_{e,f,d,g',g}^t$ and $HQ_{f,d}^{max} X_{e,f,d,g',g}^t$ are minimum and maximum hydrogen flowrate in form f by transport mode d per hour, respectively; $X^{t}_{e,f,d,g',g}$ is a binary variable indicating the flow direction of hydrogen in form f by transport mode d during time t under hydrogen scenario e from g' to g.

2.4.3 The levelized cost of hydrogen (LCOH)

The levelized cost of hydrogen (LCOH) can be derived with the above formula of HSC network optimization model as follows:

$$LCOH = \frac{C_{cot}}{AHD_{actual}} \quad (22)$$

3. CASE STUDY: HYDROGEN SUPPLY CHAIN NETWORK FOR WIM IN 2030

3.1 Description of the HSC network in WIM

The WIM is selected as a case study to verify the feasibility of the proposed model. The design of the HSC network of WIM in 2030 is shown in Fig. 2. As shown in the red ellipse in the figure, the Bayan Obo mining area is used as the production point which includes nearby large-scale geological storage. The market penetration rate of HFCV in commercial vehicles and passenger vehicles is assumed to be 7% and 3% respectively [10]. The truck transportation distance is determined according to the actual road traffic distance of Baidu map, and the pipeline transportation distance is Euclidean distance.

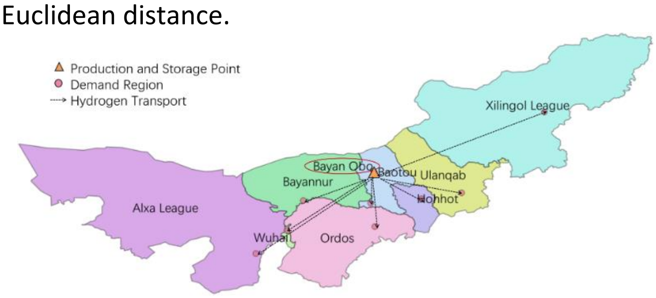

Fig. 2. Hydrogen supply chain network in WIM in 2030

3.2 Situations of Wind and Solar Resources in WIM

The WIM area is rich in wind and solar energy resources. Fig.3 illustrates the daily mean capacity factor (CF) of wind and solar power in the region in 2019 derived from the Renewables.ninja [11].

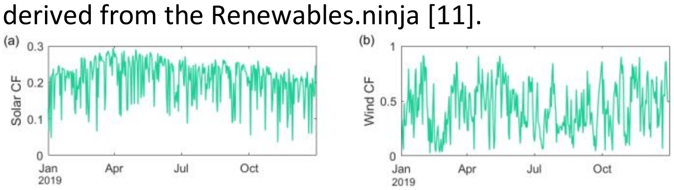

Fig. 3. Daily mean CF of wind(a) and solar(b) power generation in WIM in 2019

The annual mean CF for wind and solar power are 43.8% and 21.2%, respectively. The unit investment costs of wind turbines and photovoltaic (PV) are 945$/kW and 478$/kW respectively. In addition, the unit cost of necessary grid electricity purchase is 0.1 $/ kWh.

3.3 Techno-economic data for HSC in WIM

In this study, the outlet pressure of the electrolyzer is assumed to be 20bar [12]. The unit revenue of by-product oxygen is 0.04 $/kg [13]. The discount rate of all equipment is assumed to be 7%. The main parameters are mainly sourced from literature [12, 14-20].

4. RESULTS AND DISCUSSION

4.1 Cost of HSC network in different scenarios

After optimization calculation, total cost and LCOH of HSC with different hydrogen production and transport pathways in WIM in 2030 are shown in Fig. 4. As can be seen, the cost of LH2-Truck transportation with wind power is the lowest among the three ways, which is about 4.4$/kg. For different hydrogen production scenarios, hydrogen produced from wind power is more cost competitive than that from solar power. The reason for this is that PVs cannot generate power at night, which decreases the duty cycle of electrolysis system and increases the grid electricity purchasing cost to operate HSC network constantly. For different hydrogen supply scenarios, LH2-Truck transportation is more cost competitive. The reasons for this are that liquefaction has obvious economies of scale and the amount of LH2-Truck transportation is large.

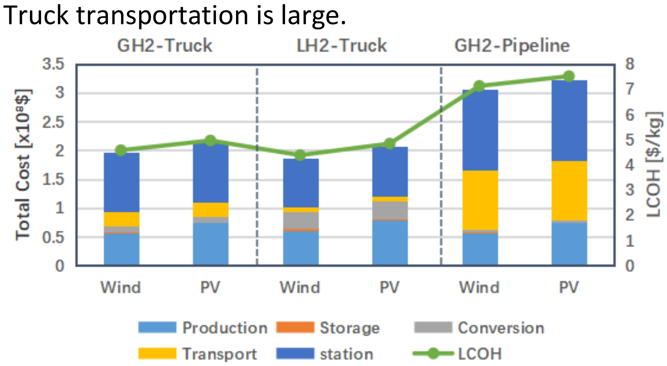

Fig. 4. Total cost and LCOH of HSC under different scenarios

Furthermore, it is worth noting that the transportation costs of the three pathways are very different. Fig. 5 illustrates the total cost and LCOH for hydrogen transport per region under different pathways in WIM in 2030. It can be seen from the figure that for different hydrogen demand and distance, the LCOH of truck transportation changes little， and the LCOH of pipeline transportation changes greatly in different regions. Especially in Wuhai, Alxa League and XilinGol League, their hydrogen demand is small and the transportation distance is long, but the pipeline transportation cost is particularly high. From the above situation, it can be predicted that the sensitivity of truck transportation to hydrogen demand and distance is less than that of pipeline transportation.

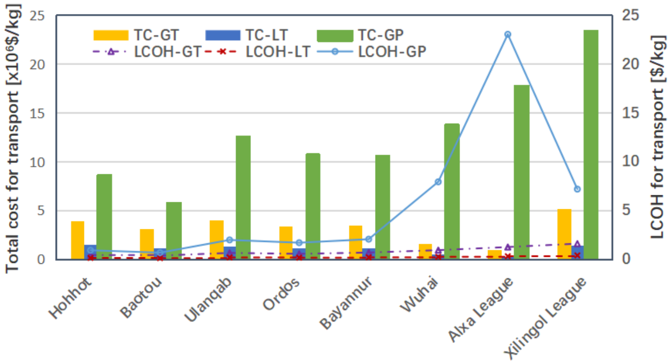

Fig. 5. Total cost and LCOH for hydrogen transport per region under different scenarios

4.2 *Influence of hydrogen demand and transportation distance on transportation cost*

In order to study the influence of hydrogen demand and transportation distance on the cost of hydrogen transportation, a detailed analysis is carried out.

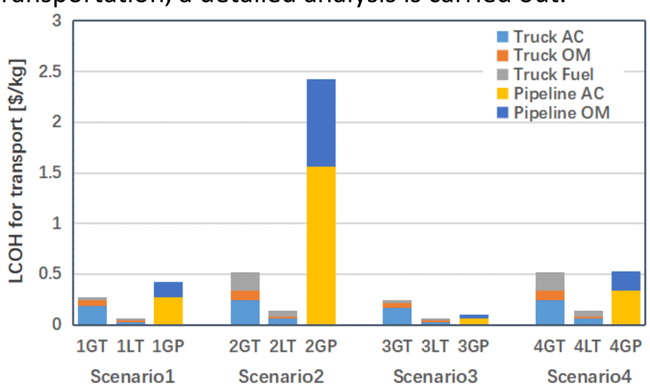

Fig. 6. The LCOH breakdown ($/kg) for the three hydrogen transport pathways

Fig. 6 shows the cost components of each transport pathway under the four demand and transport distance scenarios. The four scenarios are 15t/day, 50km; 15t/day,300km; 100t/day,50km; 100t/day,300km, from left to right. Without considering compression and liquefaction, the cost of LH2-Truck transportation is the lowest in the four scenarios and changes slightly with transportation distance, but less than GH2-Truck transportation. The change of truck transportation cost is not obvious when the demand changes. In scenario 1, 2 and 4, the cost of GH2-Pipeline transportation is the highest, and the pipeline capital cost accounts for a large proportion of 64.4%. In scenario 3, the cost of GH2-Pipeline transportation is relatively low due to large demand and short distance.

The change trend of cost with hydrogen demand and transportation distance is further analyzed below.Fig.7a shows the change trend of LCOH with hydrogen demand at 200km distance for the three hydrogen transport pathways. As can be seen, the transportation cost of GH2-Truck or LH2-Truck has little correlation with hydrogen demand. GH2-Pipeline transportation cost has great economies of scale, and it decreases rapidly with the increase of hydrogen demand. After reaching a certain scale, the cost gradually stable. This is because the capital cost of the pipeline mainly depends on the pipe diameter, which is related to the hydrogen flow.

Fig.7b shows the change trend of LCOH with hydrogen transport distance at 50t/day demand for the three hydrogen transport pathways. As can be seen, the transport distance has a great impact on the cost of GH2-Truck transportation. The reason for this is that the transport distance has a great influence on the number of trucks, fuel cost and other operation and maintenance costs. The transportation cost of LH2-Truck has a certain dependence on the transportation distance, but it is not as large as the GH2-Truck. This is due to the large capacity of the LH2-Truck. There is a great correlation between pipeline cost and transportation distance. The reason is that the transportation distance has a great influence on its capital cost.

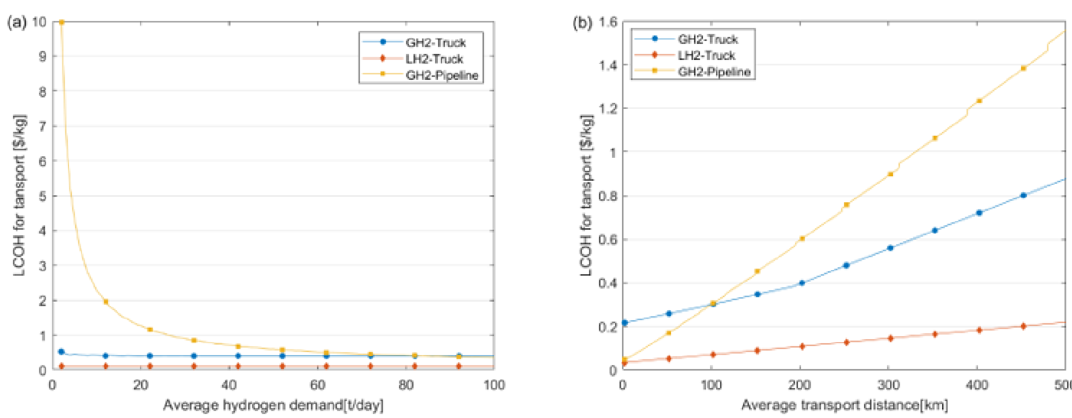

Fig. 7. (a) Effect of hydrogen demand on LCOH for transport; (b) Effect of transport distance on LCOH for transport

5. CONCLUSION

This paper constructed a HSC network model and applied it to China's WIM region. The least-cost way of green hydrogen production and delivery pathways in 2030 was obtained by dynamic programming. The results show that the combination of wind power, geological storage and LH2-Truck transportation is the least-cost HSC.

Regarding different hydrogen production sources, wind power is more cost competitive than solar energy. In terms of transportation cost, LH2-Truck transportation is the least cost option, while the cost for pipeline transportation is relatively higher. Truck transportation of compressed gaseous hydrogen or liquid hydrogen is not sensitive to hydrogen demand and has no economies of scale. However, the cost for truck transportation of compressed gaseous hydrogen is closely related to transport distance. By contrast, the transportation cost for liquid hydrogen is relatively less closely related to transport distance. Due to the capital cost factor, pipeline transportation is highly dependent on hydrogen demand and transport distance.

The current study laid a firm basis for developing a cost-effective green HSC network in the WIM region, and other regions in the world.

ACKNOWLEDGEMENT

This work was supported by Shandong University Seed Fund Program for International Research Cooperation.

AUTHOR CONTRIBUTION

L.H. and H.L. contributed equally to the genesis and conduct of this research and to the writing of the resulting manuscript.

REFERENCE

[1] BP. Energy Outlook 2020 edition. <https://www. bp.com/en/global/corporate/energy-economics/energy -outlook.html >.

[2] Almansoori A. and A. Betancourt-Torcat. Design of optimization model for a hydrogen supply chain under emission constraints - A case study of Germany. Energy, 2016. 111: 414-429.

[3] Kim M. and J. Kim. An integrated decision support model for design and operation of a wind-based hydrogen supply system. International Journal of Hydrogen Energy, 2017. 42(7): 3899-3915.

[4] Won W., et al. Design and operation of renewable energy sources based hydrogen supply system: Technology integration and optimization. Renewable Energy, 2017. 103: 226-238.

[5] Tlili O., et al. Geospatial modelling of the hydrogen infrastructure in France in order to identify the most suited supply chains. International Journal of Hydrogen Energy, 2020. 45(4): 3053-3072.

[6] De-León Almaraz S., et al. Hydrogen supply chain optimization for deployment scenarios in the Midi-Pyrénées region, France. International Journal of Hydrogen Energy, 2014. 39(23): 11831-11845.

[7] Ozarslan A. Large-scale hydrogen energy storage in salt caverns. International Journal of Hydrogen Energy, 2012. 37(19): 14265-14277.

[8] Storage and transportation technology solutions selection for large-scale hydrogen energy utilization scenarios under the trend of carbon neutralization. IOP Conference Series: Earth and Environmental Science, 2021. 770(1): 012017 (8pp).

[9] Rashid M.M., et al. Hydrogen Production by Water Electrolysis: A Review of Alkaline Water Electrolysis, PEM Water Electrolysis and High Temperature Water Electrolysis. 2015.

[10] Hydrogen Industrial Technology Innovation Alliance of China. White Paper on China Hydrogen and Fuel Cell Industry (2019 edition) [in Chinese].

[11] https://www.renewables.ninja/.

[12] Argonne National Laboratory. Hydrogen and fu el cells program. Available from:< https://www.hydr ogen.energy.gov/h2a_delivery.html >.

[13] Alavandi S., J. Seaba, and G. Subbaraman. Em erging and Existing Oxygen Production Technology S can and Evaluation. 2018, Gas Technology Institute.

[14] International Energy Agency (IEA). The Future of Hydrogen. 2019; Available from: www.iea.org/rep orts/the-future-of-hydrogen.

[15] Bloomberg Finance L.P. Hydrogen Economy Outlook: Key Messages. 2020: Singapore.

[16] Buttler A. and H. Spliethoff. Current status of water electrolysis for energy storage, grid balancing and sector coupling via power-to-gas and power-to-liquids: A review. Renew. Sustain. Energy Rev, 2018. 82: 2440-2454.

[17] US DOE. The Fuel Cell Technologies Office Multi-Year Research, Development, and Demonstration Plan. 2016, Technical report: US Department of Energy.

[18] Reuß M., et al. Seasonal storage and alternative carriers: A flexible hydrogen supply chain model. Applied Energy, 2017. 200: 290-302.

[19] https://www.globalpetrolprices.com/China/.

[20] IEA G20 Hydrogen report: Assumptions. < https://www.iea.org/corrections >.